

On the Singularity Induced by Boundary Conditions in a Third-Order Thick Plate Theory

C. S. Huang

Associate Professor,
Department of Civil Engineering,
National Chiao Tung University,
1001 Ta-Hsueh Road,
Taiwan 30050, R. O. C.
e-mail: cshuang@cc.nctu.edu.tw

This paper thoroughly examines the singularity of stress resultants of the form $r^{-\xi}F(\theta)$ for $0 < \xi \leq 1$ as $r \rightarrow 0$ (Williams-type singularity) at the vertex of an isotropic thick plate; the singularity is caused by homogeneous boundary conditions around the vertex. An eigenfunction expansion is applied to derive the first known asymptotic solution for displacement components, from the equilibrium equations of Reddy's third-order shear deformation plate theory. The characteristic equations for determining the singularities of stress resultants are presented for ten sets of boundary conditions. These characteristic equations are independent of the thickness of the plate, Young's modulus, and shear modulus, but some do depend on Poisson's ratio. The singularity orders of stress resultants for various boundary conditions are expressed in graphic form as a function of the vertex angle. The characteristic equations obtained herein are compared with those from classic plate theory and first-order shear deformation plate theory. Comparison results indicate that different plate theories yield different singular behavior for stress resultants. Only the vertex with simply supported radial edges (S(I)-S(I) boundary condition) exhibits the same singular behavior according to all these three plate theories.

[DOI: 10.1115/1.1490371]

Introduction

Obtaining accurate numerical solutions to many elasticity problems requires knowledge of the singular behavior of stress components in the neighborhood of singular points in the domain of the problem under consideration. For example, analyzing crack (or V-notch) problems using finite element approaches usually involves shape functions to describe correctly the singular behavior of stresses at the crack tip ([1,2]). The admissible functions of the Ritz method include the corner functions that precisely describe the moment singularities at the notches or corners in vibration problems of thin plates with V-notches or with re-entrant corners, to accelerate convergence and increase the accuracy of the solution ([3,4]).

Many papers have addressed the stress singularities at sharp corners based on plane elasticity theory (i.e., [5–8]) and three-dimensional elasticity theory ([9,10]). However, the stress singularities for different plate theories have received lesser attention. Williams [11] first investigated the stress singularities due to boundary conditions in the angular corner of isotropic thin plates under bending. Williams and Owens [12] and Williams and Chapkis [13] extended this work to thin plates with varying flexural rigidity and with polarly orthotropic material properties, respectively. Rao [14] considered the singularities at the interface corners for bi-material thin plates, and Ojikutu, Low, and Scott [15] investigated stress singularities at the apex of a laminated composite thin plate with simply supported radial edges. Huang et al. [16] discussed the singularities of moments and shear forces at the apex of a sector plate with simply supported radial edges in an exact solution for vibrations of such a plate. Sinclair [17] considered logarithmic stress singularities in thin plate theory.

Based on the first-order shear deformation plate theory, Burton

and Sinclair [18] investigated the stress singularities at corners due to six sets of homogeneous boundary conditions by introducing a stress potential. Huang et al. [19] examined the singularities of moments and shear forces at the vertex of a Mindlin sector plate with simply supported radial edges, by establishing an exact solution in terms of Bessel functions for the vibrations of such a plate. Recently, Huang [20] comprehensively investigated the stress singularities of moments and shear forces at corners caused by ten sets of homogeneous boundary conditions by adopting Xie and Chaudhuri's technique ([10]) to directly solve the equilibrium equations in terms of displacement components. Comparing the results with the exact solution given by Huang et al. [19] reveals that the singularity orders for moments and shear forces in Huang's results ([20]) are consistent with those in the exact solution for a simply supported corner, while the solution proposed by Burton and Sinclair [18] is consistent only for moment singularities but not for shear force singularities.

Comparing published work based on classical plate theory and on first-order shear deformation plate theory reveals that different singularity orders for moments and shear forces are suggested by different plate theories. Consequently, this study aims primarily to investigate for the first time, what results are suggested by the third-order shear deformation thick plate theory. This study applies Reddy's refined plate theory ([21]). The theory is equivalent to other third-order shear deformation plate theories proposed by Schmidt [22] and Krishna Murty [23]. This work considers only the Williams-type stress singularities at a corner caused by various boundary conditions but does not consider logarithmic stress singularities as the former singularities are more often encountered than the latter. The eigenfunction expansion methodology proposed by Hartranft and Sih [9] for three-dimensional elasticity problems is adopted to determine the asymptotic displacement field around the corner by solving the equilibrium equations in terms of displacement components in Reddy's refined plate theory. The characteristic equations for determining the singularity orders of stress resultants are established for ten sets of boundary conditions around a corner. Finally, the singular behavior of stress resultants obtained in this investigation is compared with those determined from the classic plate theory, first-order shear deformation plate theory, and three-dimensional elasticity theory.

Contributed by the Applied Mechanics Division of THE AMERICAN SOCIETY OF MECHANICAL ENGINEERS for publication in the ASME JOURNAL OF APPLIED MECHANICS. Manuscript received by the ASME Applied Mechanics Division, July 11, 2001; final revision, Feb. 28, 2002. Associate Editor: R. C. Benson. Discussion on the paper should be addressed to the Editor, Prof. Robert M. McMeeking, Department of Mechanical and Environmental Engineering University of California—Santa Barbara, Santa Barbara, CA 93106-5070, and will be accepted until four months after final publication of the paper itself in the ASME JOURNAL OF APPLIED MECHANICS.

Basic Formulation

For a sector plate with cylindrical coordinates shown in Fig. 1, the displacement field for the third-order plate theory proposed by Reddy [21] is given as

$$u = z \left[\psi_r - \frac{4}{3} \left(\frac{z}{h} \right)^2 (\psi_r + w_{,r}) \right], \quad (1)$$

$$v = z \left[\psi_\theta - \frac{4}{3} \left(\frac{z}{h} \right)^2 \left(\psi_\theta + \frac{1}{r} w_{,\theta} \right) \right], \quad (2)$$

$$w = w(r, \theta), \quad (3)$$

where the subscript “ j ” refers to a partial differential with respect to independent variable j ; u , v , and w denote the displacements of a point (r, θ, z) along the r , θ , and z directions, while ψ_r and ψ_θ are the rotations of the midplane normal in the radial and circumferential directions, respectively. This displacement field leads to zero shear stresses, σ_{zr} and $\sigma_{z\theta}$, on the plate top and bottom surfaces.

By using the variational method, one can develop the equilibrium equations and consistent boundary conditions. The equilibrium equations without external loading in terms of the stress resultants are

$$C_1 \left(P_{r,rr} + \frac{2}{r} P_{r,r} + \frac{1}{r^2} P_{\theta,\theta\theta} - \frac{1}{r} P_{\theta,r} + \frac{2}{r} P_{r\theta,r\theta} + \frac{2}{r^2} P_{r\theta,\theta} \right) + \frac{\bar{Q}_r}{r} + \bar{Q}_{r,r} + \frac{1}{r} \bar{Q}_{\theta,\theta} = 0, \quad (4)$$

$$\bar{M}_{r,r} + \frac{\bar{M}_r}{r} - \frac{\bar{M}_\theta}{r} + \frac{1}{r} \bar{M}_{r\theta,\theta} - \bar{Q}_r = 0, \quad (5)$$

$$\frac{1}{r} \bar{M}_{\theta,\theta} + \bar{M}_{r\theta,r} + \frac{2\bar{M}_{r\theta}}{r} - \bar{Q}_\theta = 0, \quad (6)$$

$C_1 = 4/3h^2$, $C_2 = 4/h^2$, $\bar{M}_{r\theta} = M_{r\theta} - C_1 P_{r\theta}$, $\bar{M}_\beta = M_\beta - C_1 P_\beta$, $\bar{Q}_\beta = Q_\beta - C_2 R_\beta$, h is the thickness of plate and subscript β denotes r or θ . Furthermore, the radial boundary conditions (at $\theta = \alpha$) should specify

$$\psi_\theta \text{ or } \bar{M}_\theta, \quad \psi_r \text{ or } \bar{M}_{r\theta},$$

$$w \text{ or } \bar{Q}_\theta + C_1 \left(\frac{2}{r} P_{r\theta} + 2P_{r\theta,r} + \frac{1}{r} P_{\theta,\theta} \right), \text{ and } \frac{w_{,\theta}}{r} \text{ or } P_\theta. \quad (7)$$

The circumferential boundary conditions (at $r=R$) should prescribe

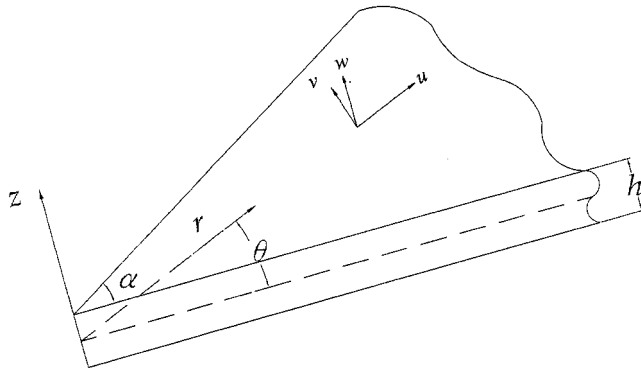


Fig. 1 Coordinate system and positive displacement components for a sector plate

$$\psi_\theta \text{ or } \bar{M}_{r\theta}, \quad \psi_r \text{ or } \bar{M}_r,$$

$$w \text{ or } \bar{Q}_r + C_1 \left(\frac{P_r}{r} + P_{r,r} + \frac{2}{r} P_{r\theta,\theta} - \frac{P_\theta}{r} \right), \text{ and } w_{,r} \text{ or } P_r. \quad (8)$$

The details of derivation for the equilibrium equations and boundary conditions in Cartesian coordinates can be found in Reddy's book [24]. The stress resultants in above equations are related to stress components by

$$\begin{Bmatrix} Q_\beta \\ R_\beta \end{Bmatrix} = \int_{-h/2}^{h/2} \sigma_{\beta z} \begin{Bmatrix} 1 \\ z \end{Bmatrix} dz, \quad (9a)$$

$$\begin{Bmatrix} M_\beta \\ P_\beta \end{Bmatrix} = \int_{-h/2}^{h/2} \sigma_{\beta\beta} \begin{Bmatrix} z \\ z^3 \end{Bmatrix} dz, \quad (9b)$$

$$\begin{Bmatrix} M_{r\theta} \\ P_{r\theta} \end{Bmatrix} = \int_{-h/2}^{h/2} \sigma_{r\theta} \begin{Bmatrix} z \\ z^3 \end{Bmatrix} dz. \quad (9c)$$

For an isotropic and elastic plate, the relationships between the stress resultants and displacement components are established by using strain-displacement and stress-strain relationships. They are

$$Q_r = \frac{2Gh}{3} (\psi_r + w_{,r}), \quad Q_\theta = \frac{2Gh}{3} \left(\psi_\theta + \frac{1}{r} w_{,\theta} \right),$$

$$R_r = \frac{Gh^3}{30} (\psi_r + w_{,r}), \quad R_\theta = \frac{Gh^3}{30} \left(\psi_\theta + \frac{1}{r} w_{,\theta} \right),$$

$$M_{r\theta} = Gh^3 \left[\frac{1}{12} \left(\psi_{\theta,r} - \frac{1}{r} \psi_\theta + \frac{1}{r} \psi_{r,\theta} \right) - \frac{1}{60r} \left(-\psi_\theta - \frac{2}{r} w_{,\theta} + \psi_{r,\theta} + 2w_{,r\theta} + r\psi_{\theta,r} \right) \right],$$

$$M_r = \frac{Eh^3}{1-\nu^2} \left\{ \left(\frac{1}{15} \psi_{r,r} - \frac{1}{60} w_{,rr} \right) + \frac{\nu}{r} \left[\frac{1}{15} (\psi_r + \psi_{\theta,\theta}) - \frac{1}{60} \left(w_{,r} + \frac{1}{r} w_{,\theta\theta} \right) \right] \right\},$$

$$M_\theta = \frac{Eh^3}{1-\nu^2} \left\{ \frac{1}{r} \left[\frac{1}{15} (\psi_r + \psi_{\theta,\theta}) - \frac{1}{60} \left(w_{,r} + \frac{1}{r} w_{,\theta\theta} \right) \right] + \nu \left(\frac{1}{15} \psi_{r,r} - \frac{1}{60} w_{,rr} \right) \right\},$$

$$P_{r\theta} = \frac{Gh^5}{1680} \left[16\psi_{\theta,r} - \frac{16}{r} \psi_\theta + \frac{16}{r} \psi_{r,\theta} - \frac{10}{r} \left(w_{,r\theta} - \frac{w_{,\theta}}{r} \right) \right],$$

$$P_r = \frac{Eh^2}{(1-\nu^2)} \left\{ \frac{\psi_{r,r}}{105} - \frac{w_{,rr}}{336} + \frac{\nu}{r} \left[\frac{1}{80} (\psi_r + \psi_{\theta,\theta}) - \frac{1}{336} \left(\psi_{\theta,\theta} + \psi_r + w_{,r} + \frac{w_{,\theta\theta}}{r} \right) \right] \right\},$$

$$P_\theta = \frac{Eh^2}{(1-\nu^2)} \left\{ \frac{1}{r} \left[\frac{1}{105} (\psi_r + \psi_{\theta,\theta}) - \frac{1}{336} \left(w_{,r} + \frac{w_{,\theta\theta}}{r} \right) \right] + \nu \left(\frac{\psi_{r,r}}{105} - \frac{w_{,rr}}{336} \right) \right\}, \quad (10)$$

where E is Young's modulus; G is the shear modulus, and ν is Poisson's ratio.

Substituting Eq. (10) into Eqs. (4)–(6) with careful arrangement yields the equilibrium equations in terms of the displacement components:

$$\begin{aligned} \psi_{r,rrr} + \frac{2}{r} \psi_{r,rr} + \frac{1}{r^2} \psi_{r,r\theta\theta} + \frac{1}{r^3} \psi_{r,\theta\theta} - \frac{1}{r^2} \psi_{r,r} + \frac{1}{r^3} \psi_r + \frac{1}{r^3} \psi_{\theta,\theta\theta\theta} \\ + \frac{1}{r} \psi_{\theta,rr\theta} - \frac{1}{r^2} \psi_{\theta,r\theta} + \frac{1}{r^3} \psi_{\theta,\theta} - \frac{5}{16} \left(w_{rrrr} + \frac{2}{r} w_{rrr} \right. \\ \left. + \frac{2}{r^2} w_{rr\theta\theta} - \frac{1}{r^2} w_{r,r} - \frac{2}{r^3} w_{r,\theta\theta} + \frac{1}{r^3} w_{r,r} + \frac{1}{r^4} w_{\theta\theta\theta\theta} \right. \\ \left. + \frac{4}{r^4} w_{\theta\theta} \right) + \frac{21(1-\nu)}{h^2} \left(\psi_{r,r} + \frac{1}{r} \psi_r + \frac{1}{r} \psi_{\theta,\theta} + w_{rr} + \frac{1}{r} w_{r,r} \right. \\ \left. + \frac{1}{r^2} w_{\theta\theta} \right) = 0, \end{aligned} \quad (11)$$

$$\begin{aligned} \psi_{r,rr} + \left(\frac{1}{r} \psi_r \right)_{,r} + \frac{1-\nu}{2} \frac{1}{r^2} \psi_{r,\theta\theta} - \frac{3-\nu}{2} \frac{1}{r^2} \psi_{\theta,r} + \frac{1+\nu}{2} \frac{1}{r} \psi_{\theta,r\theta} \\ - \frac{4}{17} \left(w_{rrr} + \frac{1}{r} w_{rr} + \frac{1}{r^2} w_{r,\theta\theta} - \frac{1}{r^2} w_{r,r} - \frac{2}{r^3} w_{\theta\theta} \right) \\ - \frac{84(1-\nu)}{17h^2} (\psi_r + w_{r,r}) = 0, \end{aligned} \quad (12)$$

$$\begin{aligned} \frac{1+\nu}{2} \frac{1}{r} \psi_{r,r\theta} + \frac{3-\nu}{2} \frac{1}{r^2} \psi_{r,\theta} + \frac{1-\nu}{2} \psi_{\theta,rr} + \frac{1-\nu}{2} \left(\frac{1}{r} \psi_{\theta} \right)_{,r} \\ + \frac{1}{r^2} \psi_{\theta,\theta\theta} - \frac{4}{17} \left(\frac{1}{r} w_{rr\theta} + \frac{1}{r^2} w_{r,\theta} + \frac{1}{r^3} w_{\theta\theta\theta} \right) \\ - \frac{84(1-\nu)}{17h^2} \left(\psi_{\theta} + \frac{1}{r} w_{r,\theta} \right) = 0. \end{aligned} \quad (13)$$

Construction of Series Solution

The eigenfunction expansion approach proposed by Hartrant and Sih [9] for three-dimensional elasticity problems is adopted herein to find the solution of Eqs. (11)–(13). The displacement components can be expressed in terms of the following series:

$$w(r, \theta) = \sum_{m=0}^{\infty} \sum_{n=0,2}^{\infty} r^{\lambda_m+n+1} W_n^{(m)}(\theta, \lambda_m), \quad (14a)$$

$$\psi_r(r, \theta) = \sum_{m=0}^{\infty} \sum_{n=0,2}^{\infty} r^{\lambda_m+n} \Psi_n^{(m)}(\theta, \lambda_m), \quad (14b)$$

$$\psi_{\theta}(r, \theta) = \sum_{m=0}^{\infty} \sum_{n=0,2}^{\infty} r^{\lambda_m+n} \Phi_n^{(m)}(\theta, \lambda_m), \quad (14c)$$

where the characteristic values λ_m are assumed to be constants and can be complex numbers. Notably, odd n in Eqs. (14) will not produce any additional solution such that they are not considered in Eqs. (14).

The real part of λ_m must exceed zero to satisfy the regularity conditions at the vertex of the sector plate. The regularity conditions require that ψ_{θ} , ψ_r , w , and w_r are finite as r approaches zero. As a result, the solution form given in Eqs. (14) with the real part of λ_m less than one leads to singularities of M_r , M_{θ} , $M_{r\theta}$, P_r , P_{θ} , and $P_{r\theta}$, which is observed from the relationships between stress resultants and displacement components given in Eq. (10). However, no singularity for shear forces (Q_r and Q_{θ}), R_r and R_{θ} will be produced from the solution.

Substituting Eqs. (14) into Eqs. (11)–(13) yields

$$\begin{aligned} \sum_{m=0}^{\infty} \sum_{n=0,2}^{\infty} r^{\lambda_m+n-3} \left\{ (\lambda_m n + 1) \Psi_n^{(m)} + (\lambda_m + n - 1)^2 (\lambda_m + n + 1) \right. \\ \left. \times \Psi_n^{(m)} + \Phi_{n,\theta\theta\theta}^{(m)} + (\lambda_m + n - 1)^2 \Phi_{n,\theta}^{(m)} - \frac{5}{16} [(\lambda_m + n - 1)^2 \right. \\ \left. + (\lambda_m + n + 1)^2 W_n^{(m)} + 2((\lambda_m + n)^2 + 1) W_{n,\theta\theta}^{(m)} + W_{n,\theta\theta\theta\theta}^{(m)}] \right\} \\ + \frac{21(1-\nu)}{h^2} r^{\lambda_m+n-1} \{ (\lambda_m + n + 1) \Psi_n^{(m)} + \Phi_{n,\theta}^{(m)} + W_{n,\theta\theta}^{(m)} \\ + (\lambda_m + n + 1)^2 W_n^{(m)} \} = 0 \end{aligned} \quad (15)$$

$$\begin{aligned} \sum_{m=0}^{\infty} \sum_{n=0,2}^{\infty} r^{\lambda_m+n-2} \left\{ \frac{1-\nu}{2} \Psi_{n,\theta\theta}^{(m)} + [(\lambda_m + n)^2 - 1] \Psi_n^{(m)} \right. \\ \left. + \left[\frac{1+\nu}{2} (\lambda_m + n) - \frac{3-\nu}{2} \right] \Phi_{n,\theta}^{(m)} - \frac{4}{17} [(\lambda_m + n + 1)^2 \right. \\ \left. \times (\lambda_m + n - 1) W_n^{(m)} + (\lambda_m + n - 1) W_{n,\theta\theta}^{(m)}] \right. \\ \left. - \frac{84(1-\nu)}{17h^2} r^{\lambda_m+n} \{ \Psi_n^{(m)} + (\lambda_m + n + 1) W_n^{(m)} \} \right\} = 0, \end{aligned} \quad (16)$$

$$\begin{aligned} \sum_{m=0}^{\infty} \sum_{n=0,2}^{\infty} r^{\lambda_m+n-2} \left\{ \left[\frac{1+\nu}{2} (\lambda_m + n) + \frac{3-\nu}{2} \right] \Psi_{n,\theta}^{(m)} + \Phi_{n,\theta\theta}^{(m)} \right. \\ \left. + \frac{1-\nu}{2} [(\lambda_m + n)^2 - 1] \Phi_{n,\theta}^{(m)} - \frac{4}{17} [(\lambda_m + n + 1)^2 W_{n,\theta}^{(m)} \right. \\ \left. + W_{n,\theta\theta\theta}^{(m)}] - \frac{84(1-\nu)}{17h^2} r^{\lambda_m+n} \{ \Phi_{n,\theta}^{(m)} + W_{n,\theta}^{(m)} \} \right\} = 0. \end{aligned} \quad (17)$$

Satisfying Eqs. (15)–(17) leads to the coefficients of r with different orders equal to zero. Subsequently, a set of recurrent relationships among $W_n^{(m)}$, $\Psi_n^{(m)}$, $\Phi_n^{(m)}$ and their previous values can be attained and expressed as

$$\begin{aligned} (\lambda_m + n + 3) \Psi_{n+2,\theta\theta}^{(m)} + (\lambda_m + n + 1)^2 (\lambda_m + n + 3) \Psi_{n+2}^{(m)} + \Phi_{n+2,\theta\theta\theta}^{(m)} \\ + (\lambda_m + n + 1)^2 \Phi_{n+2,\theta}^{(m)} - \frac{5}{16} [(\lambda_m + n + 1)^2 (\lambda_m + n + 3)^2 \\ \times W_{n+2}^{(m)} + 2((\lambda_m + n + 2)^2 + 1) W_{n+2,\theta\theta}^{(m)} + W_{n+2,\theta\theta\theta\theta}^{(m)}] \\ = - \frac{21(1-\nu)}{h^2} \{ (\lambda_m + n + 1) \Psi_n^{(m)} + \Phi_{n,\theta}^{(m)} + W_{n,\theta\theta}^{(m)} \\ + (\lambda_m + n + 1)^2 W_n^{(m)} \}, \end{aligned} \quad (18)$$

$$\begin{aligned} [(\lambda_m + n + 2)^2 - 1] \Psi_{n+2}^{(m)} + \frac{1-\nu}{2} \Psi_{n+2,\theta\theta}^{(m)} - \frac{3-\nu}{2} \Phi_{n+2,\theta}^{(m)} \\ + \frac{1+\nu}{2} (\lambda_m + n + 2) \Phi_{n+2,\theta}^{(m)} - \frac{4}{17} [(\lambda_m + n + 3)^2 \\ \times (\lambda_m + n + 1) W_{n+2}^{(m)} + (\lambda_m + n + 1) W_{n+2,\theta\theta}^{(m)}] \\ = \frac{84(1-\nu)}{17h^2} [\Psi_n^{(m)} + (\lambda_m + n + 1) W_n^{(m)}], \end{aligned} \quad (19)$$

$$\begin{aligned} \left[\frac{1+\nu}{2} (\lambda_m + n + 2) + \frac{3-\nu}{2} \right] \Psi_{n+2,\theta}^{(m)} + \frac{1-\nu}{2} [(\lambda_m + n + 2)^2 - 1] \\ \times \Phi_{n+2}^{(m)} + \Phi_{n+2,\theta\theta}^{(m)} - \frac{4}{17} [(\lambda_m + n + 3)^2 W_{n+2,\theta}^{(m)} + W_{n+2,\theta\theta\theta}^{(m)}] \\ = \frac{84(1-\nu)}{17h^2} (\Phi_n^{(m)} + W_{n,\theta}^{(m)}). \end{aligned} \quad (20)$$

Furthermore, one can establish the following equations from the coefficients of the lowest order of r in Eqs. (15)–(17):

$$(\lambda_m + 1)\Psi_{0,\theta\theta}^{(m)} + (\lambda_m - 1)^2(\lambda_m + 1)\Psi_0^{(m)} + \Phi_{0,\theta\theta\theta}^{(m)} + (\lambda_m - 1)^2\Phi_{0,\theta}^{(m)} - \frac{5}{16}[(\lambda_m - 1)^2(\lambda_m + 1)^2W_0^{(m)} + 2(\lambda_m^2 + 1)W_{0,\theta\theta}^{(m)} + W_{0,\theta\theta\theta}^{(m)}] = 0, \quad (21)$$

$$(\lambda_m^2 - 1)\Psi_0^{(m)} + \frac{1-\nu}{2}\Psi_{0,\theta\theta}^{(m)} - \frac{3-\nu}{2}\Phi_{0,\theta}^{(m)} + \frac{(1+\nu)\lambda_m}{2}\Phi_{0,\theta\theta}^{(m)} - \frac{4}{17}[(\lambda_m + 1)^2(\lambda_m - 1)W_0^{(m)} + (\lambda_m - 1)W_{0,\theta\theta}^{(m)}] = 0, \quad (22)$$

$$\left(\frac{(1+\nu)\lambda_m}{2} + \frac{3-\nu}{2}\right)\Psi_{0,\theta}^{(m)} + \frac{1-\nu}{2}(\lambda_m^2 - 1)\Phi_0^{(m)} + \Phi_{0,\theta\theta}^{(m)} - \frac{4}{17}[(\lambda_m + 1)^2W_{0,\theta}^{(m)} + W_{0,\theta\theta\theta}^{(m)}] = 0. \quad (23)$$

It is easy to find that the general solution for the set of ordinary differential equations given by Eqs. (21)–(23) is

$$\Phi_0^{(m)}(\theta, \lambda_m) = B_0 \cos(\lambda_m + 1)\theta + B_1 \sin(\lambda_m + 1)\theta + B_2 \cos(\lambda_m - 1)\theta + B_3 \sin(\lambda_m - 1)\theta, \quad (24a)$$

$$\Psi_0^{(m)}(\theta, \lambda_m) = -B_1 \cos(\lambda_m + 1)\theta + B_0 \sin(\lambda_m + 1)\theta + A_2 \cos(\lambda_m - 1)\theta + A_3 \sin(\lambda_m - 1)\theta, \quad (24b)$$

$$W_0^{(m)}(\theta, \lambda_m) = A_0 \cos(\lambda_m + 1)\theta + A_1 \sin(\lambda_m + 1)\theta + (k_1A_2 + k_2B_3)\cos(\lambda_m - 1)\theta + (k_1A_3 - k_2B_2)\sin(\lambda_m - 1)\theta, \quad (24c)$$

where

$$k_1 = \frac{17}{16\lambda_m} \left(\frac{(1+\nu)\lambda_m}{2} + \frac{3-\nu}{2} \right),$$

$$k_2 = \frac{17}{16\lambda_m} \left(\frac{(1+\nu)\lambda_m}{2} - \frac{3-\nu}{2} \right),$$

and A_i and B_i ($i=1,2,3,4$) are coefficients to be determined from boundary conditions.

To establish the complete series solution for equilibrium equations (i.e., Eqs. (11)–(13)), one has to determine λ_m and the relations among A_i and B_i in Eqs. (24) from the boundary conditions along radial edges. Then, one finds the solutions for $\Phi_n^{(m)}$, $\Psi_n^{(m)}$, and $W_n^{(m)}$ with $n > 1$ from Eqs. (18)–(20) and boundary conditions.

Notably, one may construct the series solution by starting with assuming the following solution form:

$$w(r, \theta) = \sum_{m=0}^{\infty} \sum_{n=0,2}^{\infty} r^{\lambda_m+n+l_1} \bar{W}_n^{(m)}(\theta, \lambda_m), \quad (25a)$$

$$\psi_r(r, \theta) = \sum_{m=0}^{\infty} \sum_{n=0,2}^{\infty} r^{\lambda_m+n+l_2} \bar{\Psi}_n^{(m)}(\theta, \lambda_m), \quad (25b)$$

$$\psi_\theta(r, \theta) = \sum_{m=0}^{\infty} \sum_{n=0,2}^{\infty} r^{\lambda_m+n+l_3} \bar{\Phi}_n^{(m)}(\theta, \lambda_m), \quad (25c)$$

where l_i ($i=1,2,3$) can be arbitrary integers, but at least one of them is zero. Following the above procedure, one will find the solution form given by Eqs. (14) is the only one that may yield Williams-type stress singularities. Furthermore, there are possible

solutions involving logarithmic function of r leading to logarithmic singularities for stress resultants at the vertex of a sector plate, which are out of the scope of this work and will not be investigated here. The readers who are interested in the logarithmic singularities may refer to Dempsey and Sinclair [7] and Sinclair [17].

Characteristic Equations and Corner Functions

To determine Williams-type stress singularities at the vertex of a sector plate caused by homogeneous boundary conditions, one only needs the asymptotic solution with the lowest order of r in the series solution of Eqs. (14). Consequently, only the solution with $n=0$ in Eqs. (14) needs to be considered. Let

$$\psi_{\theta 0}^{(m)} = r^{\lambda_m} \Phi_0^{(m)}(\theta, \lambda_m), \quad \psi_{r 0}^{(m)} = r^{\lambda_m} \Psi_0^{(m)}(\theta, \lambda_m), \quad \text{and} \quad w_0^{(m)} = r^{\lambda_m+1} W_0^{(m)}(\theta, \lambda_m). \quad (26)$$

Furthermore, as well known, the stress singularities are affected by the boundary conditions along radial edges only.

In the following, we will consider four types of homogeneous boundary conditions along a radial edge, say $\theta = \alpha$, namely,

$$\text{clamped: } w = \psi_r = \psi_\theta = \frac{w, \theta}{r} = 0, \quad (27a)$$

$$\text{free: } \bar{M}_\theta = \bar{M}_{r,\theta} = \bar{Q}_\theta + C_1 \left(\frac{2}{r} P_{r\theta} + 2P_{r,\theta,r} + \frac{1}{r} P_{\theta,\theta} \right) = P_\theta = 0, \quad (27b)$$

$$\text{type I simply supported: } w = \psi_r = \bar{M}_\theta = P_\theta = 0, \quad (27c)$$

$$\text{type II simply supported: } w = \bar{M}_\theta = \bar{M}_{r,\theta} = P_\theta = 0. \quad (27d)$$

For simplicity, C and F are used to present the clamped and free boundary conditions, respectively, while S(I) and S(II) denote type I and type II simply supported boundary conditions.

For the sake of demonstration, we will describe the procedure for obtaining the characteristic equation for λ_m , and the corresponding asymptotic displacement field for describing the singular behavior of stress resultants in the vicinity of a corner. Consider a sector plate with vertex angle equal to α and having clamped and free boundary conditions along two radial edges, respectively. For the free radial edge at $\theta = \alpha$, substituting Eq. (26) into Eq. (27b) and using the relations given in Eq. (10) leads to the following equations for the lowest order of r :

$$a_{11}A_0 + a_{12}A_1 + a_{13}A_2 + a_{14}A_3 + a_{15}B_0 + a_{16}B_1 + a_{17}B_2 + a_{18}B_3 = 0, \quad (28a)$$

$$a_{21}A_0 + a_{22}A_1 + a_{23}A_2 + a_{24}A_3 + a_{25}B_0 + a_{26}B_1 + a_{27}B_2 + a_{28}B_3 = 0, \quad (28b)$$

$$a_{31}A_0 + a_{32}A_1 + a_{33}A_2 + a_{34}A_3 + a_{35}B_0 + a_{36}B_1 + a_{37}B_2 + a_{38}B_3 = 0, \quad (28c)$$

$$a_{41}A_0 + a_{42}A_1 + a_{43}A_2 + a_{44}A_3 + a_{45}B_0 + a_{46}B_1 + a_{47}B_2 + a_{48}B_3 = 0, \quad (28d)$$

where lengthy expression for a_{ij} is given in the Appendix. Similarly, one also obtains four equations for A_i and B_i from the clamped edge at $\theta = 0$:

$$B_0 + B_2 = 0, \quad (29a)$$

$$-B_1 + A_2 = 0, \quad (29b)$$

$$A_0 + k_1A_2 + k_2B_3 = 0, \quad (29c)$$

$$(\lambda_m + 1)A_1 + (\lambda_m - 1)(k_1A_3 - k_2B_2) = 0. \quad (29d)$$

Equations (28) and (29) construct a set of linear homogeneous algebraic equations for A_i and B_i . To have nontrivial solution for A_i and B_i yields the characteristic equations for λ_m ,

$$\sin^2 \lambda_m \alpha = \frac{4 - \lambda_m^2 (1 + \nu)^2 \sin^2 \alpha}{(3 - \nu)(1 + \nu)}, \quad (30a)$$

$$\sin^2 \lambda_m \alpha = \frac{4 - \lambda_m^2 (1 - \nu)^2 \sin^2 \alpha}{(3 + \nu)(1 - \nu)}. \quad (30b)$$

Then, one can find the relations among A_i and B_i from Eqs. (29) and (28a)–(28c). Consequently, $\psi_{\theta 0}^{(m)}$, $\psi_{r 0}^{(m)}$, and $w_0^{(m)}$ in Eq. (26) are expressed as

$$\begin{aligned} \psi_{r 0}^{(m)}(r, \theta) = & B_3 r^{\lambda_m} \left\{ \frac{1 + \lambda_m}{\lambda_m - 1} \cos(\lambda_m + 1) \theta - \eta_2 \sin(\lambda_m + 1) \theta \right. \\ & \left. - \frac{1 + \lambda_m}{\lambda_m - 1} \cos(\lambda_m - 1) \theta + \eta_1 \sin(\lambda_m - 1) \theta \right\}, \end{aligned} \quad (31a)$$

$$\begin{aligned} \psi_{\theta 0}^{(m)}(r, \theta) = & B_3 r^{\lambda_m} \left\{ - \frac{1 + \lambda_m}{\lambda_m - 1} \sin(\lambda_m + 1) \theta - \eta_2 \cos(\lambda_m + 1) \theta \right. \\ & \left. + \sin(\lambda_m - 1) \theta + \eta_2 \cos(\lambda_m - 1) \theta \right\}, \end{aligned} \quad (31b)$$

$$\begin{aligned} w_0^{(m)}(r, \theta) = & B_3 r^{\lambda_m + 1} \left\{ \left(\frac{k_1(1 + \lambda_m)}{\lambda_m - 1} - k_2 \right) \cos(\lambda_m + 1) \theta \right. \\ & + \frac{(1 - \lambda_m)}{\lambda_m + 1} (k_1 \eta_1 - k_2 \eta_2) \sin(\lambda_m + 1) \theta \\ & + \left(- \frac{(1 + \lambda_m)k_1}{\lambda_m - 1} + k_2 \right) \cos(\lambda_m - 1) \theta \\ & \left. + (k_1 \eta_1 - k_2 \eta_2) \sin(\lambda_m - 1) \theta \right\}, \end{aligned} \quad (31c)$$

where η_1 and η_2 are given in Table 1. Since $\psi_{\theta 0}^{(m)}$, $\psi_{r 0}^{(m)}$, and $w_0^{(m)}$ are the smallest order of r in the series solution given in Eqs. (14) for different λ_m , they characterize the asymptotic behavior of the series solution in the vicinity of the vertex. Furthermore, they are the displacement field describing the singular behavior of stress resultants at the vertex when the positive real part of λ_m is less than one. The asymptotic displacement field will be called as corner functions below.

By following the procedure given above, one can develop the characteristic equations for λ_m and the corresponding corner functions for different boundary conditions along radial edges. Tables 1 and 2, respectively, summarize the characteristic equations for λ_m and the corresponding corner functions for ten different combinations of boundary conditions. To take advantage of the problem's symmetry, the corner functions for the identical boundary conditions along two radial edges were determined by considering the range, $-\alpha/2 \leq \theta \leq \alpha/2$, which is also indicated in Table 1.

Notably, using trigonometric identities, the characteristic equations for S(I)_S(I) in Table 2 are found equivalent to

$$\cos(\lambda_m - 1)\alpha/2 = 0 \quad \text{or} \quad \cos(\lambda_m + 1)\alpha/2 = 0, \quad (32a)$$

and

$$\sin(\lambda_m - 1)\alpha/2 = 0 \quad \text{or} \quad \sin(\lambda_m + 1)\alpha/2 = 0, \quad (32b)$$

for symmetric and antisymmetric cases, respectively. Consequently, the corner functions corresponding to the roots of λ_m for different equations are separately listed in Table 1. Similar situation also happens to the cases with S(II)_S(II) and S(I)_S(II) boundary conditions.

Singularity of Stress Resultants

The relations between displacements and stress resultants given in Eq. (10) indicate that the smallest orders of r for moments ($M_r, M_\theta, M_{r\theta}$) and $P_r, P_\theta,$ and $P_{r\theta}$ are the same, and they are

less than those for rotation components (ψ_r and ψ_θ) and w by one and two, respectively. Consequently, the root λ_m of the characteristic equations with a positive real part below one leads to singular behavior of moments and $P_r, P_\theta,$ and $P_{r\theta}$, described by $r^{\lambda_m - 1}$ as r approaches zero. Moreover, the singular behavior of stress components, $\sigma_{rr}, \sigma_{\theta\theta},$ and $\sigma_{r\theta}$, can also be found according to the relationship between stresses and displacement components in elasticity. Notably, the characteristic equations listed in Table 2 reveal that the thickness of the plate is unrelated to these characteristic equations, and Poisson's ratio is the single material property that can affect the singularity order of stress resultants.

As stated earlier, the real part of λ_m ($\text{Re}(\lambda_m)$) must exceed zero to meet the regularity conditions for the displacement components, as r approaches zero. Figure 2 displays the minimum positive values of $\text{Re}(\lambda_m)$ versus the vertex angle (α) for various boundary conditions. These minimum values of $\text{Re}(\lambda_m)$ were determined by solving the characteristic equations in Table 2 with ν equal to 0.3. Notably, some different boundary conditions around a corner produce the same minimum $\text{Re}(\lambda_m)$ within certain ranges of vertex angles. Boundary conditions S(I)_S(I), S(I)_S(II), and S(II)_S(II) give the same minimum $\text{Re}(\lambda_m)$, while boundary conditions S(I)_F and S(II)_F yield the same minimum $\text{Re}(\lambda_m)$ except for $180 \text{ deg} < \alpha < 270 \text{ deg}$. Boundary conditions C_C and F_F have the same minimum $\text{Re}(\lambda_m)$ when α exceeds 180 deg. Boundary conditions C_F and C_S(II) show the same minimum $\text{Re}(\lambda_m)$ for α below about 128 deg. When α is between 180 deg and 270 deg, boundary condition S(I)_C yield a minimum $\text{Re}(\lambda_m)$ equal to that for S(I)_F and C_S(II).

Figure 2 indicates that no singularities of moments and $P_r, P_\theta,$ and $P_{r\theta}$ occur if α is less than 60 deg, regardless of the boundary conditions around the corner. However, such singularities are always present if α exceeds 180 deg. A corner with S(I)_S(I), S(I)_S(II), S(II)_S(II), S(I)_F, S(II)_F, or S(I)_C boundary conditions exhibit a singularity when α exceeds 90 deg. Boundary conditions C_F and C_S(II) cause the strongest singularity of the stress resultants at the vertex for α between 60 deg and approximately 105 deg; S(I)_S(I), S(I)_S(II), and S(II)_S(II) boundary conditions result in the strongest singularity for other vertex angles. C_C and F_F boundary conditions cause a singularity in stress resultants for α exceeding 180 deg. This singularity is weaker than that due to other boundary conditions.

Figure 2 also indicates that singularities generally become more severe as the vertex angle increases, except in those cases with S(I)_S(I), S(I)_S(II), S(II)_S(II), C_F, or C_S(II) boundary conditions. For the C_F and C_S(II) cases, the minimum positive $\text{Re}(\lambda_m)$ increases with α for α between 122 deg and 130 deg in which region the roots of the characteristic equations change from real to complex numbers. The minimum positive $\text{Re}(\lambda_m)$ for S(I)_S(I), and S(II)_S(II) was determined from different characteristic equations for different ranges of α . That is, from Eqs. (32), when $\alpha \leq \pi$, the minimum positive $\text{Re}(\lambda_m)$ is determined from $\cos(\lambda_m + 1)\alpha/2 = 0$, while for $\pi < \alpha \leq 3\pi/2$ and for $3\pi/2 \leq \alpha < 2\pi$, the minimum positive $\text{Re}(\lambda_m)$ is determined from $\cos(\lambda_m - 1)\alpha/2 = 0$ and $\sin(\lambda_m + 1)\alpha/2 = 0$, respectively. As α approaches 2π , the singularity order for moments and $P_r, P_\theta,$ and $P_{r\theta}$ due to S(I)_S(I), S(I)_S(II), and S(II)_S(II) boundary conditions approaches r^{-1} , while F_F and C_C boundary conditions lead to an order of $r^{-3/2}$. Other boundary conditions yield an order of $r^{-3/4}$.

Most of the characteristic equations listed in Table 2 can also be found in either classic plate theory (CPT) or first-order shear deformation plate theory (FSDPT). Williams [11] obtained those characteristic equations marked with a superscript, "#," in Table 2, from the classic plate theory. Burton and Sinclair [18] and Huang [20] found those characteristic equations marked with superscript "*" in Table 2, based on FSDPT using different solution approaches. The characteristic equations pertaining to the S(II) boundary condition given in Table 2 cannot find the corresponding ones in classic plate theory because no S(II) boundary condition

Table 1 Corner functions

Case No.	Boundary Conditions	Corner Functions
1	S(I)-S(I) $\left(-\frac{\alpha}{2} \leq \theta \leq \frac{\alpha}{2}\right)$	(1) for $\cos(\lambda_m - 1)\alpha/2 = 0$ $\psi_{r_0}^{(m)}(r, \theta) = A_2 r^{\lambda_m} \cos(\lambda_m - 1)\theta$, $\psi_{\theta_0}^{(m)}(r, \theta) = B_3 r^{\lambda_m} \sin(\lambda_m - 1)\theta$, $w_0^{(m)}(r, \theta) = (k_1 A_2 + k_2 B_3) r^{\lambda_m + 1} \cos(\lambda_m - 1)\theta$
		(2) for $\cos(\lambda_m + 1)\alpha/2 = 0$ $\psi_{r_0}^{(m)}(r, \theta) = -B_1 r^{\lambda_m} \cos(\lambda_m + 1)\theta$, $\psi_{\theta_0}^{(m)}(r, \theta) = B_1 r^{\lambda_m} \sin(\lambda_m + 1)\theta$, $w_0^{(m)}(r, \theta) = A_0 r^{\lambda_m + 1} \cos(\lambda_m + 1)\theta$
		(3) for $\sin(\lambda_m - 1)\alpha/2 = 0$ $\psi_{r_0}^{(m)}(r, \theta) = A_3 r^{\lambda_m} \sin(\lambda_m - 1)\theta$, $\psi_{\theta_0}^{(m)}(r, \theta) = B_2 r^{\lambda_m} \cos(\lambda_m - 1)\theta$, $w_0^{(m)}(r, \theta) = (k_1 A_3 + k_2 B_2) r^{\lambda_m + 1} \sin(\lambda_m - 1)\theta$
		(4) for $\sin(\lambda_m + 1)\alpha/2 = 0$ $\psi_{r_0}^{(m)}(r, \theta) = B_0 r^{\lambda_m} \sin(\lambda_m + 1)\theta$, $\psi_{\theta_0}^{(m)}(r, \theta) = B_0 r^{\lambda_m} \cos(\lambda_m + 1)\theta$, $w_0^{(m)}(r, \theta) = A_1 r^{\lambda_m + 1} \sin(\lambda_m + 1)\theta$
2	C-F $(0 \leq \theta \leq \alpha)$	$\psi_{r_0}^{(m)}(r, \theta) = B_3 r^{\lambda_m} \left\{ \frac{1 + \lambda_m}{\lambda_m - 1} \cos(\lambda_m + 1)\theta - \eta_2 \sin(\lambda_m + 1)\theta - \frac{1 + \lambda_m}{\lambda_m - 1} \cos(\lambda_m - 1)\theta + \eta_1 \sin(\lambda_m - 1)\theta \right\}$
		$\psi_{\theta_0}^{(m)}(r, \theta) = B_3 r^{\lambda_m} \left\{ -\frac{1 + \lambda_m}{\lambda_m - 1} \sin(\lambda_m + 1)\theta - \eta_2 \cos(\lambda_m + 1)\theta + \sin(\lambda_m - 1)\theta + \eta_2 \cos(\lambda_m - 1)\theta \right\}$
		$w_0^{(m)}(r, \theta) = B_3 r^{\lambda_m + 1} \left\{ \left(\frac{k_1(1 + \lambda_m)}{\lambda_m - 1} - k_2 \right) \cos(\lambda_m + 1)\theta + \frac{(1 - \lambda_m)}{\lambda_m + 1} (k_1 \eta_1 - k_2 \eta_2) \sin(\lambda_m + 1)\theta + \left(-\frac{(1 + \lambda_m)k_1}{\lambda_m - 1} + k_2 \right) \cos(\lambda_m - 1)\theta + (k_1 \eta_1 - k_2 \eta_2) \sin(\lambda_m - 1)\theta \right\}$ $\eta_1 = \frac{(\lambda_m + 1)[(3 + \nu + \nu\lambda_m - \lambda_m)\cos(\lambda_m - 1)\alpha + (1 + \lambda_m)(1 - \nu)\cos(\lambda_m + 1)\alpha]}{(\lambda_m - 1)[(3 + \nu + \nu\lambda_m - \lambda_m)\sin(\lambda_m - 1)\alpha - (1 - \lambda_m)(1 - \nu)\sin(\lambda_m + 1)\alpha]}$ $\eta_2 = \frac{(3 + \nu + \nu\lambda_m - \lambda_m)\cos(\lambda_m - 1)\alpha + (1 + \lambda_m)(1 - \nu)\cos(\lambda_m + 1)\alpha}{(3 + \nu + \nu\lambda_m - \lambda_m)\sin(\lambda_m - 1)\alpha - (1 - \lambda_m)(1 - \nu)\sin(\lambda_m + 1)\alpha}$
3	S(I)-F $(0 \leq \theta \leq \alpha)$	$\psi_{r_0}^{(m)}(r, \theta) = B_2 r^{\lambda_m} \left\{ \eta_3 \sin(\lambda_m + 1)\theta + \frac{\lambda_m + 1}{\lambda_m - 1} \sin(\lambda_m - 1)\theta \right\}$, $\psi_{\theta_0}^{(m)}(r, \theta) = B_2 r^{\lambda_m} \{ \eta_3 \cos(\lambda_m + 1)\theta + \cos(\lambda_m - 1)\theta \}$
		$w_0^{(m)}(r, \theta) = B_2 r^{\lambda_m + 1} \left\{ \eta_4 \sin(\lambda_m + 1)\theta + \left[\frac{(\lambda_m + 1)k_1}{\lambda_m - 1} - k_2 \right] \sin(\lambda_m - 1)\theta \right\}$ $\eta_3 = -\frac{(3 + \nu - \lambda_m + \nu\lambda_m) \sin(\lambda_m - 1)\alpha}{(\nu - 1)(\lambda_m - 1) \sin(\lambda_m + 1)\alpha}$, $\eta_4 = \frac{17}{4(\lambda_m + 1)} \eta_3$
4	S(I)-C $(0 \leq \theta \leq \alpha)$	$\psi_{r_0}^{(m)}(r, \theta) = B_0 r^{\lambda_m} \left\{ \sin(\lambda_m + 1)\theta - \frac{\sin(\lambda_m + 1)\alpha}{\sin(\lambda_m - 1)\alpha} \sin(\lambda_m - 1)\theta \right\}$
		$\psi_{\theta_0}^{(m)}(r, \theta) = B_0 r^{\lambda_m} \left\{ \cos(\lambda_m + 1)\theta - \frac{\cos(\lambda_m + 1)\alpha}{\cos(\lambda_m - 1)\alpha} \cos(\lambda_m - 1)\theta \right\}$ $w_0^{(m)}(r, \theta) = B_0 r^{\lambda_m + 1} \left\{ \eta_5 \sin(\lambda_m + 1)\theta + \left[-\frac{k_1 \sin(\lambda_m + 1)\alpha}{\sin(\lambda_m - 1)\alpha} + \frac{k_2 \cos(\lambda_m + 1)\alpha}{\cos(\lambda_m - 1)\alpha} \right] \sin(\lambda_m - 1)\theta \right\}$ $\eta_5 = k_1 - \frac{k_2(\sin 2\lambda_m \alpha - \sin 2\alpha)}{(\sin 2\lambda_m \alpha + \sin 2\alpha)}$
5	F-F $\left(-\frac{\alpha}{2} \leq \theta \leq \frac{\alpha}{2}\right)$	(1) Symmetric case $\psi_{r_0}^{(m)}(r, \theta) = B_3 r^{\lambda_m} \left\{ \eta_7 \cos(\lambda_m + 1)\theta + \frac{1 + \lambda_m}{1 - \lambda_m} \cos(\lambda_m - 1)\theta \right\}$, $\psi_{\theta_0}^{(m)}(r, \theta) = B_3 r^{\lambda_m} \{ -\eta_7 \sin(\lambda_m + 1)\theta + \sin(\lambda_m - 1)\theta \}$ $w_0^{(m)}(r, \theta) = B_3 r^{\lambda_m + 1} \left\{ \eta_6 \cos(\lambda_m + 1)\theta + \left(\frac{(1 + \lambda_m)k_1}{1 - \lambda_m} + k_2 \right) \cos(\lambda_m - 1)\theta \right\}$ $\eta_6 = \frac{17 \eta_7}{4(1 + \lambda_m)}$, $\eta_7 = \frac{3 + \nu - \lambda_m + \lambda_m \nu}{(-1 + \nu)(\lambda_m - 1)} \frac{\cos(\lambda_m - 1)\alpha/2}{\cos(\lambda_m + 1)\alpha/2}$
		(2) Antisymmetric case $\psi_{r_0}^{(m)}(r, \theta) = B_2 r^{\lambda_m} \left\{ -\eta_9 \sin(\lambda_m + 1)\theta + \frac{\lambda_m + 1}{\lambda_m - 1} \sin(\lambda_m - 1)\theta \right\}$, $\psi_{\theta_0}^{(m)}(r, \theta) = B_2 r^{\lambda_m} \{ -\eta_9 \cos(\lambda_m + 1)\theta + \cos(\lambda_m - 1)\theta \}$

Table 2 Characteristic equations for high-order shear deformation plate theory

Case No.	Boundary Conditions	Characteristic Equations
1	S(I)-S(I)	Symmetric: $\cos \lambda_m \alpha = -\cos \alpha^{*,\#}$ Antisymmetric: $\cos \lambda_m \alpha = +\cos \alpha^{*,\#}$
2	C_F	$\sin^2 \lambda_m \alpha = \frac{4 - \lambda_m^2 (1 + \nu)^2 \sin^2 \alpha^*}{(3 - \nu)(1 + \nu)}$ $\sin^2 \lambda_m \alpha = \frac{4 - \lambda_m^2 (1 - \nu)^2 \sin^2 \alpha^\#}{(3 + \nu)(1 - \nu)}$
3	S(I)_F	$\sin 2\lambda_m \alpha = \lambda_m \sin 2\alpha^*$ $\sin 2\lambda_m \alpha = \frac{\lambda_m(1 - \nu)}{-3 - \nu} \sin 2\alpha^\#$
4	S(I)_C	$\sin 2\lambda_m \alpha = \frac{\lambda_m(1 + \nu)}{-3 + \nu} \sin 2\alpha^*$ $\sin 2\lambda_m \alpha = \lambda_m \sin 2\alpha^\#$
5	F_F	Symmetric: $\sin \lambda_m \alpha = -\lambda_m \sin \alpha^{*,*}$ $\sin \lambda_m \alpha = -\frac{\lambda_m(1 - \nu)}{-3 - \nu} \sin \alpha^\#$ Antisymmetric: $\sin \lambda_m \alpha = \lambda_m \sin \alpha^{*,*}$ $\sin \lambda_m \alpha = \frac{\lambda_m(1 - \nu)}{-3 - \nu} \sin \alpha^\#$
6	C_C	Symmetric: $\sin \lambda_m \alpha = -\frac{\lambda_m(1 + \nu)}{-3 + \nu} \sin \alpha^{*,*}$ $\sin \lambda_m \alpha = -\lambda_m \sin \alpha^\#$ Antisymmetric: $\sin \lambda_m \alpha = \frac{\lambda_m(1 + \nu)}{-3 + \nu} \sin \alpha^{*,*}$ $\sin \lambda_m \alpha = \lambda_m \sin \alpha^\#$
7	S(II)_S(II)	Symmetric: $\sin \lambda_m \alpha = -\lambda_m \sin \alpha^{*,*} \cos \lambda_m \alpha = -\cos \alpha$ Antisymmetric: $\sin \lambda_m \alpha = \lambda_m \sin \alpha^{*,*} \cos \lambda_m \alpha = \cos \alpha$
8	C_S(II)	$\sin^2 \lambda_m \alpha = \frac{4 - \lambda_m^2 (1 + \nu)^2 \sin^2 \alpha^*}{(3 - \nu)(1 + \nu)}$ $\sin 2\lambda_m \alpha = \lambda_m \sin 2\alpha$
9	S(I)_S(II)	$\sin 2\lambda_m \alpha = \lambda_m \sin 2\alpha^*$ $\cos 2\lambda_m \alpha = \cos 2\alpha$
10	S(II)_F	$\sin \lambda_m \alpha = \pm \lambda_m \sin \alpha^*$ $\sin 2\lambda_m \alpha = \frac{\lambda_m(-1 + \nu)}{3 + \nu} \sin 2\alpha$

Note: * means that the equation can be recovered in FSDPT.
means that the equation can be recovered in CPT.

any condition around the vertex. In both cases, $\alpha = 300\text{deg}$ and $\nu = 0.3$. The value of λ_m is real in the case of the F_F boundary condition, and λ_m is complex for the C_F condition. The stress resultants were computed by substituting the corresponding corner functions given in Table 1 into Eq. (10) and setting the undetermined coefficients (such as B_3 in Table 1) in the corner functions equal to unity. Notably, when λ_m is a complex number, the corresponding stress resultants are also complex functions. Figure 4 only presents the distributions for the imaginary parts of the stress resultants. In Fig. 4, the superscripts “+” and “-” in the legend

of the vertical axis are the signs for the stress resultants. Positive stress resultants were plotted as $\text{Log}|M^+/D|$ versus $\text{Log}r$ and negative stress resultants were plotted as $\text{Log}|M^-/D|$ versus $\text{Log}r$, where D is the flexural rigidity.

Figure 3 shows that the magnitudes of the stress resultants from the present solution monotonically approach infinity as r approaches zero, because λ_m is a positive real number and smaller than unity. Figure 3 also displays the stress resultant distributions obtained by CPT and by FSDPT. The stress resultant distributions for FSDPT were computed using the corner functions given in [20], and the distributions for CPT were obtained from the corner functions given in [25] and [26]. The coefficients to be determined in the corner functions for CPT and FSDPT were obtained by requiring that the values of M_r at $r = 10^{-5}$ for CPT and FSDPT should be identical to that from the present solution. The value of r was arbitrarily chosen. Consequently, the distribution of M_r for FSDPT coincides with that for the theory used here because both theories have the same λ_m in this case. However, the distributions of M_θ for these two theories are not coincident (Fig. 3). In fact, the distributions of stress resultants along various values of θ , determined by these two theories, are generally not coincident, which fact is not depicted here. Therefore, although the theory used here and FSDPT have the same λ_m for the case shown in Fig. 3, the stress resultants approach infinity at different rates for each theory as r approaches zero. This may be due to the fact that $M_{r\theta}$ is required to equal zero along a free edge in FSDPT, whereas $M_{r\theta}$ for the theory used here still approaches infinity as r approaches zero, even along a free edge. The stress resultants for CPT approach infinity more slowly than those for FSDPT and the theory used here as r approaches zero, since the value of λ_m for CPT exceeds those for the other two theories.

Figure 4 reveals that the stress resultants from the present solution oscillate toward infinitely as r goes to zero because λ_m is complex. Figure 4 also plots the distributions of stress resultants for CPT and FSDPT. The corner function for FSDPT given in [20] and the corner function for CPT given in [4] and [26] were used to determine these distributions. The undetermined coefficients in these corner functions were obtained in the same way as for Fig. 3. Notably, λ_m for CPT equals that for the theory used here in the case of Fig. 4. Figure 4 indicates that the distributions of stress resultants from the present solution coincide with those for CPT. Stress resultant functions of M_r , M_θ , and $M_{r\theta}$ from the present solution can be shown to be exactly the same as those for CPT in this case. The value of λ_m for FSDPT is also a complex number but differs from those for CPT and the theory used here. Accordingly, the distributions of stress resultants for FSDPT significantly differ from those for CPT and the theory used here.

The present solution involves no singularities for shear forces or R_β , which is attributable to the regularity conditions at $r = 0$ and the relations between stress resultants and displacement components. The regularity conditions require ψ_θ , ψ_r , w , and w_r to remain finite as r approaches zero. The relations in Eq. (10) suggest that the shear forces and R_β either have the same order of r as ψ_θ or ψ_r , or one order lower than w . Consequently, shear forces and R_β cannot exhibit singular behavior as r approaches zero, regardless of the boundary conditions around the vertex. Notably, this finding markedly differs from that observed in CPT and FSDPT. Since shear deformation is not considered in CPT, shear forces are determined from equilibrium equations such that the singularity of shear forces is always stronger than that for moments. Huang [20] found the characteristic equations for the singularity of shear forces in first-order shear deformation plate theory, according to which the singularity order of shear forces also depends on both the boundary conditions and the vertex angle.

Comparing the singular behavior in various plate theories with that in elasticity theory yields interesting results. Hartranft and Sih [9] developed the characteristic equations for a completely free

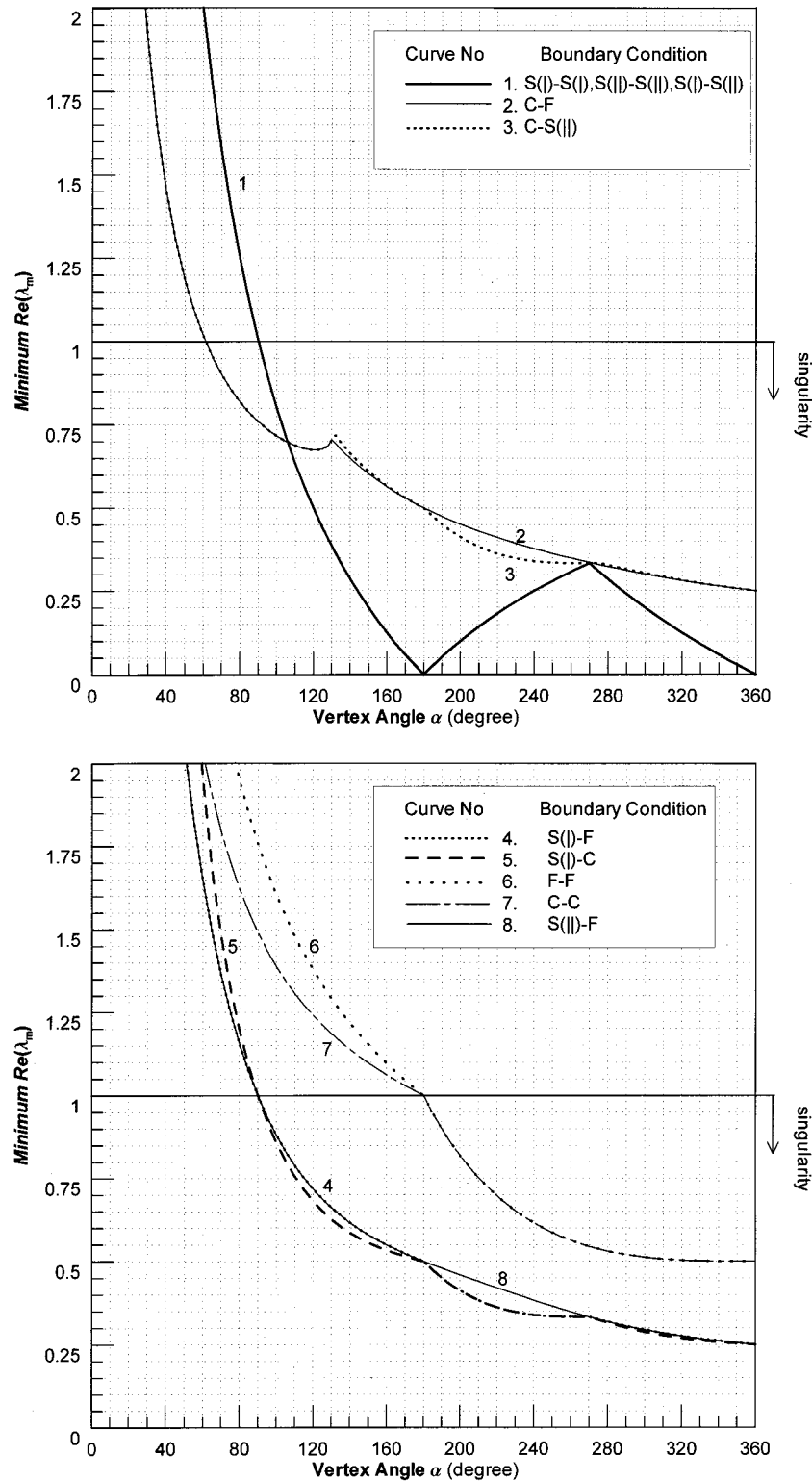


Fig. 2 Variation of minimum $\text{Re}(\lambda_m)$ with vertex angle

wedge based on a three-dimensional elasticity approach. According to their results, the stress singularity order of r at the vertex of the wedge is $\lambda_m - 1$, where λ_m is determined by

$$\sin \lambda_m \alpha = \lambda_m \sin \alpha, \quad (33a)$$

$$\sin \lambda_m \alpha = -\lambda_m \sin \alpha, \quad (33b)$$

$$\text{or } \lambda_m = (2m + 1)\pi / \alpha, \quad (33c)$$

where $m = 0, 1, 2, 3, \dots$. The first two equations also appear in the present work for F-F boundary conditions (Table 2), while none of these equations are found in CPT [11]. However, all three equations are also found in FSDPT [20]. The third equation characterizes the singular behavior of shear forces in FSDPT.

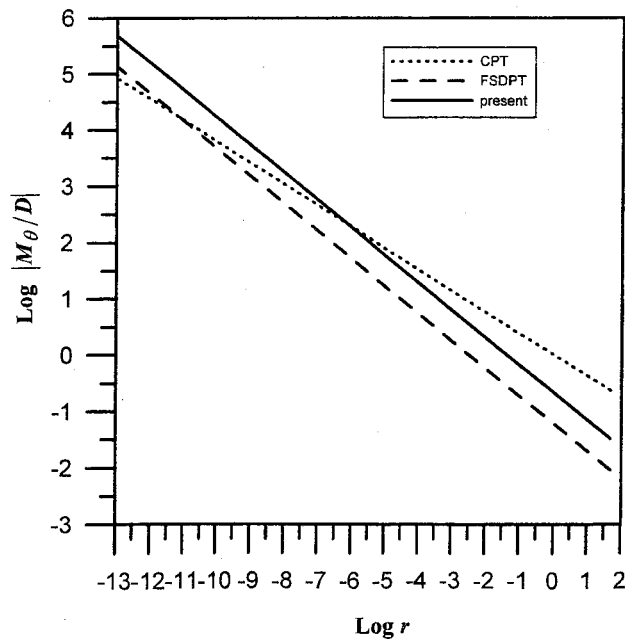
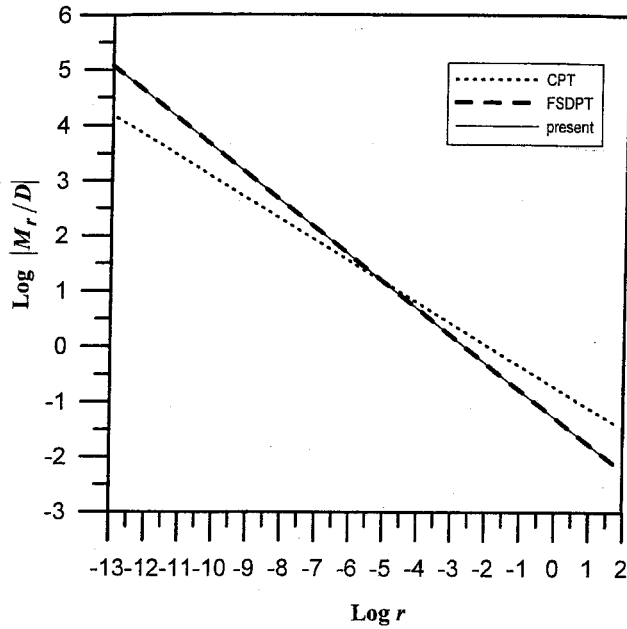


Fig. 3 Distribution of M_r and M_θ along the symmetric axis for a wedge with free radial edges

Concluding Remarks

This study has established the asymptotic displacement field to describe the singular behavior of stress resultants at the vertex of a sector thick plate based on Reddy's third-order thick plate theory. The solution was obtained using an eigenfunction expansion approach to solve the equilibrium equations in terms of displacement components. The characteristic equations for determining Williams-type singularities of stress resultants were also developed for ten sets of boundary conditions around the vertex. These characteristic equations do not involve the thickness of plate. Poisson's ratio is the single material property that could possibly influence the singular behavior of stress resultants. Notably, unlike the singularity of shear forces found in classic plate theory and first-order shear deformation plate theory, no such singularity is involved in Reddy's plate theory.

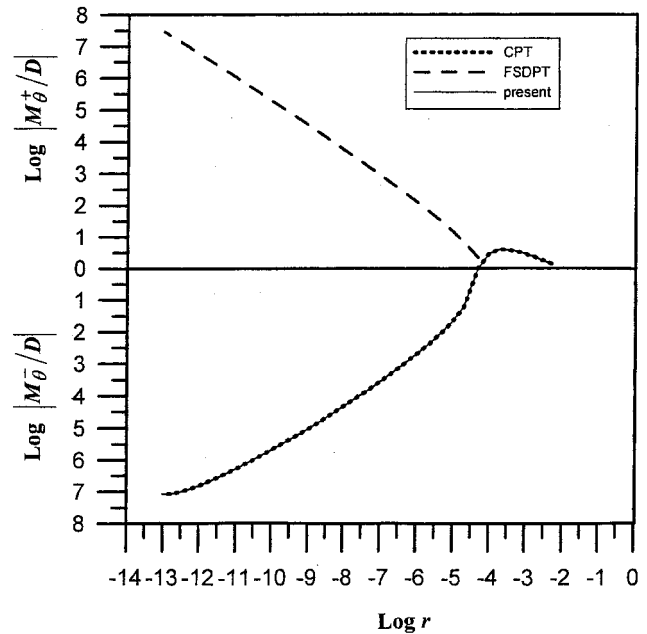
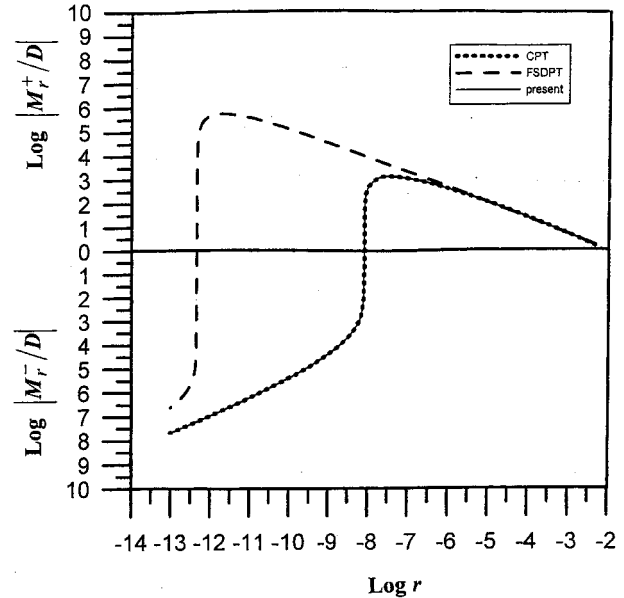


Fig. 4 Distributions of M_r and $M_\theta = \alpha/2$ for a wedge with C_F boundary conditions

The characteristic equations for determining the singular behavior of M_r , M_θ , $M_{r\theta}$, P_r , P_θ , and $P_{r\theta}$ in this work include the characteristic equations for classic plate theory and first-order shear deformation plate theory. For the same boundary conditions, different plate theories usually lead to different singularity orders for stress resultants, except for the case with S(I)_S(I) boundary conditions. For a plate with $\nu = 0.3$, no singularity occurs when the vertex angle is less than 60 deg, while a singularity is always present when the vertex angle exceeds 180 deg. C_F boundary conditions result in the strongest singularity among the ten sets of boundary conditions considered in this study when the vertex angle is less than approximately 105 deg, while S(I)_S(I), S(II)_S(II), and S(I)_S(II) boundary conditions lead to the strongest singularity for other angles. F_F and C_C boundary conditions cause the weakest singularity.

The singularity orders for stress resultants and the corresponding corner functions given in this investigation are important for

developing singularity elements in finite element approach for complex thick plate problems involving corner stress singularities. Furthermore, the corner functions for various corner boundary conditions provided herein are also very valuable for applying the Ritz method to solve thick plate problems with reentrant corners like the work by McGee et al. [4] and Leissa et al. [3] for thin plate problems.

Acknowledgments

This work reported herein was supported by the National Science Council, R.O.C. through research grant no. NSC90-2211-E-009-035. The supported is gratefully acknowledged. The appreciation is also extended to author's graduate students, Mr. M. J. Chang and Mr. I. P. Hung, for preparing the figures shown in the paper.

Appendix

The coefficients for Eqs. (28) are

$$\begin{aligned}
 a_{11} &= 5\lambda_m(1+\lambda_m)\cos(1+\lambda_m)\alpha, \\
 a_{12} &= 5\lambda_m(1+\lambda_m)\sin(1+\lambda_m)\alpha, \\
 a_{13} &= \frac{\rho_1}{\nu-1}\cos(1-\lambda_m)\alpha, \quad a_{14} = -\frac{\rho_1}{\nu-1}\sin(1-\lambda_m)\alpha, \\
 a_{15} &= -16\lambda_m\sin(1+\lambda_m)\alpha, \\
 a_{16} &= 16\lambda_m\cos(1+\lambda_m)\alpha, \quad a_{17} = \frac{\rho_2}{\nu-1}\sin(1-\lambda_m)\alpha, \\
 a_{18} &= \frac{\rho_2}{\nu-1}\cos(1-\lambda_m)\alpha \\
 a_{21} &= (\nu-1)\lambda_m(1+\lambda_m)\cos(1+\lambda_m)\alpha, \\
 a_{22} &= (\nu-1)\lambda_m(1+\lambda_m)\sin(1+\lambda_m)\alpha \\
 a_{23} &= \delta_1\cos(1-\lambda_m)\alpha, \quad a_{24} = -\delta_1\sin(1-\lambda_m)\alpha, \\
 a_{25} &= -4(\nu-1)\lambda_m\sin(1+\lambda_m)\alpha, \\
 a_{26} &= 4(\nu-1)\lambda_m\cos(1+\lambda_m)\alpha, \quad a_{27} = \delta_2\sin(1-\lambda_m)\alpha, \\
 a_{28} &= \delta_2\cos(1-\lambda_m)\alpha, \\
 a_{31} &= 8\lambda_m(1+\lambda_m)\sin(1+\lambda_m)\alpha, \\
 a_{32} &= -8\lambda_m(1+\lambda_m)\cos(1+\lambda_m)\alpha, \\
 a_{33} &= -(\lambda_m-1)(-17+8k_1\lambda_m)\sin(1-\lambda_m)\alpha, \\
 a_{34} &= -(\lambda_m-1)(-17+8k_1\lambda_m)\cos(1-\lambda_m)\alpha, \\
 a_{35} &= 34\lambda_m\cos(1+\lambda_m)\alpha, \quad a_{36} = 34\lambda_m\sin(1+\lambda_m)\alpha, \\
 a_{37} &= (\lambda_m-1)(17+8k_2\lambda_m)\cos(1-\lambda_m)\alpha, \\
 a_{38} &= -(\lambda_m-1)(17+8k_2\lambda_m)\sin(1-\lambda_m)\alpha \\
 a_{41} &= -\gamma_1\sin(1+\lambda_m)\alpha, \quad a_{42} = \gamma_1\cos(1+\lambda_m)\alpha, \\
 a_{43} &= -\gamma_2\sin(1-\lambda_m)\alpha, \\
 a_{44} &= -\gamma_2\cos(1-\lambda_m)\alpha, \quad a_{45} = -\gamma_3\cos(1+\lambda_m)\alpha, \\
 a_{46} &= -\gamma_3\sin(1+\lambda_m)\alpha, \\
 a_{47} &= -\gamma_4\cos(1-\lambda_m)\alpha, \quad a_{48} = \gamma_4\sin(1-\lambda_m)\alpha \\
 \rho_1 &= -16(1+\nu\lambda_m)+5k_1\lambda_m(3+\nu-\lambda_m+\nu\lambda_m), \\
 \rho_2 &= 16+(-16+5(3+\nu)k_2)\lambda_m+5(\nu-1)k_2\lambda_m^2, \\
 \delta_1 &= -4(1+\nu\lambda_m)+(3+\nu-\lambda_m+\nu\lambda_m)k_1\lambda_m,
 \end{aligned}$$

$$\delta_2 = 4 + (-4 + (3 + \nu)k_2)\lambda_m + (\nu - 1)k_2\lambda_m^2,$$

$$\gamma_1 = 5(\nu - 1)E\lambda_m(1 + \lambda_m)(1 - \lambda_m),$$

$$\gamma_2 = E(\lambda_m - 1)\lambda_m[2(-1 + \nu)(-8 + 5k_1\lambda_m) + 16(1 + \nu\lambda_m) - 5k_1\lambda_m(3 + \nu - \lambda_m + \nu\lambda_m)],$$

$$\gamma_3 = 16(\nu - 1)E\lambda_m(1 - \lambda_m),$$

$$\gamma_4 = E(\lambda_m - 1)[16 + (-16 + 15k_2 + 5\nu k_2 - 16(\nu - 1))\lambda_m - 5(\nu - 1)k_2\lambda_m^2].$$

References

- [1] Rice, J. R., and Tracy, D. M., 1973, "Computational Fracture Mechanics," *Numerical and Computer Methods in Structural Mechanics*, S. J. Fenves et al., eds., Academic Press, San Diego, CA, pp. 585–623.
- [2] Aminpour, M. A., and Holsapple, K. A., 1991, "Finite Element Solutions for Propagating Interface Cracks With Singularity Elements," *Eng. Fract. Mech.*, **39**(3), pp. 451–468.
- [3] Leissa, A. W., McGee, O. G., and Huang, C. S., 1993, "Vibrations of Sectorial Plates Having Corner Stress Singularities," *ASME J. Appl. Mech.*, **60**, pp. 134–140.
- [4] McGee, O. G., Leissa, A. W., and Huang, C. S., 1992, "Vibrations of Cantilevered Skewed Plates With Corner Stress Singularities," *Int. J. Numer. Methods Eng.*, **35**(2), pp. 409–424.
- [5] William, M. L., 1952, "Stress Singularities Resulting From Various Boundary Conditions in Angular Corners of Plates in Extension," *ASME J. Appl. Mech.*, **19**, pp. 526–528.
- [6] Hein, V. L., and Erdogan, F., 1971, "Stress Singularities in a Two-Material Wedge," *Int. J. Fract. Mech.*, **7**(3), pp. 317–330.
- [7] Dempsey, J. P., and Sinclair, G. B., 1979, "On the Stress Singularities in the Plate Elasticity of the Composite Wedge," *J. Elast.*, **9**(4), pp. 373–391.
- [8] Ting, T. C. T., and Chou, S. C., 1981, "Edge Singularities in Anisotropic Composites," *Int. J. Solids Struct.*, **17**(11), pp. 1057–1068.
- [9] Hartranft, R. J., and Sih, G. C., 1969, "The Use of Eigenfunction Expansions in the General Solution of Three-Dimensional Crack Problems," *J. Math. Mech.*, **19**(2), pp. 123–138.
- [10] Xie, M., and Chaudhuri, R. A., 1998, "Three-Dimensional Stress Singularity at a Bimaterial Interface Crack Front," *Compos. Struct.*, **40**(2), pp. 137–147.
- [11] William, M. L., 1952, "Stress Singularities Resulting From Various Boundary Conditions in Angular Corners of Plates Under Bending," *Proceedings of 1st U.S. National Congress of Applied Mechanics*, ASME, New York, pp. 325–329.
- [12] Williams, M. L., and Owens, R. H., 1954, "Stress Singularities in Angular Corners of Plates Having Linear Flexural Rigidities for Various Boundary Conditions," *Proceedings of 2nd U.S. National Congress of Applied Mechanics*, ASME, New York, pp. 407–411.
- [13] William, M. L., and Chapkis, R. L., 1958, "Stress Singularities for a Sharp-Notched Polarly Orthotropic Plate," *Proceedings of 3rd U.S. National Congress of Applied Mechanics*, ASME, New York, pp. 281–286.
- [14] Rao, A. K., 1971, "Stress Concentrations and Singularities at Interfaces Corners," *Z. Angew. Math. Mech.*, **51**, pp. 395–406.
- [15] Ojikutu, I. O., Low, R. O., and Scott, R. A., 1984, "Stress Singularities in Laminated Composite Wedge," *Int. J. Solids Struct.*, **20**(8), pp. 777–790.
- [16] Huang, C. S., Leissa, A. W., and McGee, O. G., 1993, "Exact Analytical Solutions for the Vibrations of Sectorial Plates With Simply-Supported Radial Edges," *ASME J. Appl. Mech.*, **60**, pp. 478–483.
- [17] Sinclair, G. B., 2000, "Logarithmic Stress Singularities Resulting From Various Boundary Conditions in Angular Corners of Plates Under Bending," *ASME J. Appl. Mech.*, **67**, pp. 219–223.
- [18] Burton, W. S., and Sinclair, G. B., 1986, "On the Singularities in Reissner's Theory for the Bending of Elastic Plates," *ASME J. Appl. Mech.*, **53**, pp. 220–222.
- [19] Huang, C. S., McGee, O. G., and Leissa, A. W., 1994, "Exact Analytical Solutions for the Vibrations of Mindlin Sectorial Plates With Simply Supported Radial Edges," *Int. J. Solids Struct.*, **31**(11), pp. 1609–1631.
- [20] Huang, C. S., 2001, "Stress Singularities at Angular Corners in First-Order Shear Deformation Plate Theory," *Int. J. Mech. Sci.*, submitted for publication.
- [21] Reddy, J. N., 1999, *Theory and Analysis of Elastic Plates*, Taylor and Francis, London.
- [22] Schmidt, R., 1977, "A Refined Nonlinear Theory for Plates With Transverse Shear Deformation," *J. Indust. Math. Soc.*, **27**(1), pp. 23–38.
- [23] Krishna Murty, A. V., 1977, "Higher Order Theory for Vibration of Thick Plates," *AIAA J.*, **15**(2), pp. 1823–1824.
- [24] Reddy, J. N., 1984, *Energy and Variational Methods in Applied Mechanics*, John Wiley and Sons, New York.
- [25] Leissa, A. W., McGee, O. G., and Huang, C. S., 1993, "Vibrations of Circular Plates Having V-Notches or Sharp Radial Cracks," *J. Sound Vib.*, **161**(2), pp. 227–239.
- [26] Huang, C. S., 1991, "Singularities in Plate Vibration Problems," Ph.D. dissertation, The Ohio State University.